Alternative design of high torque density two- phase brushless direct current motor

Saeed Abareshi[1], Jawad Faiz[2], Mehrage Ghods[3]

[1,2,3]School of Electrical and Computer Engineering, College of Engineering, University of Tehran, Tehran, Iran

This paper proposes a design of a dual-stator brushless direct current (BLDC) motor, which has a particularly high torque density. BLDC motors are known for their high torque capacity and power density characteristics, and therefore, they are used in many applications. The proposed BLDC motor is a two-phase motor with two stators, and each stator is excited by only one phase. The duty cycle of inverter switches is complete and coils are continuously excited. Due to the full and uninterrupted use of the all coils and core, this motor has a higher torque density compared to other BLDCs. After extracting the mathematical model of the proposed motor for its better understanding, it is designed. the performance of the designed motor is analyzed using finite element analysis.

Keywords: Brushless direct current, dual stator, high torque density, high power density.

I. INTRODUCTION

The brushless direct current (BLDC) motor has been used and rapidly developed in various applications such as home appliances, electric vehicles, medical equipment, spacecraft, and submarines. BLDC motors have many advantages over conventional DC motors, induction motors, and PM motors. These advantages include good speed/torque characteristics, high dynamic response, high efficiency, long life, and noiseless operation, simple drive circuit, cheap sensors, high-speed range. In addition high power/size ratio of this motor makes it possible to use them where space and weight are critical factors [1], [2].

The BLDC motors have no mechanical brush but commutation is done electronically by switching. The duty cycle of switches is determined based on the structure and number of phases. However, in most structures, the switching duty cycle is not complete, which causes the coils and motor core not to be used optimally. Some reasons for this are explained in the following section. In single-phase BLDC motors, there are null-points in their torque waveform, so, it is impossible to start the motor in such regions. To overcome this problem,

non-uniform structures are used, which eliminate the null-points areas by adjusting the cogging torque. In these non-uniform structures, the optimal switching duty cycle is not complete [3], [4]. However, two-phase BLDC motors have been paid less attention. Various developed designs have been presented in [5], [6], in which an motor has been designed with the only-pull drive technique. Another designs introduced in [7], in which the range of inverter switch is not complete. In the

structures of three-phase and multi-phase BLDC motors, the rotor pole does not completely match the stator pole, and the optimal duty cycle of the switches is less than 2/3 or 120º [8], [9].

It is possible to apply a complete duty cycle in some structures such as single-phase BLDC motor [3], whose duty cycle is complete; however, because of its special structure, it has a low torque. Also, it is possible to apply a full duty cycle in three-phase motors [10], [11], but due to their distributed winding, in half of a period, one tooth develops torque and in the other half another tooth does it, so, they develop a relatively small torque.

The conduction range in the single-phase motors presented in [12]–[14] is complete. But the inductance of the coils at high speeds increases and the phase current rises slowly leading to a phase difference with the back EMF. This increases the torque fluctuations and decreases the average torque. This problem is solved using the advanced phase commutation technique, which matches the phases of the current and back EMF with the time change of the inverter switches [2], [12]. Another disadvantage of these structures is that existing back EMF and current harmonics, which cause higher core losses at high frequencies. Therefore, the paper has examined the harmonics.

This paper introduces an alternative structure by combining two single-phase BLDC motors. In this case, zero torque regions are eliminated, and the full-duty cycle of the switches is applied. The mathematical model of the operation of the motor is explained and its performance is predicted. Then, the motor is designed and simulated by finite element method and the results show its high torque density. The introduced dual stator motor is compared with that presented in [15] with the same dimensions and their performances are compared.

II. MATHEMATICAL MODEL AND OPERATION OF TWO-PHASE BLDC MOTOR

A. Operation

A BLDC motor rotates as a result of the interaction between its PM field at the rotor and a magnetic field generated by a DC voltage applied to its stator coils. To maintain rotation, the orientation of the stator magnetic field has to be rotated sequentially. Moreover, to deliver a higher power and torque which is ideally free from ripple, the desired rectangular AC waveform of back EMF and current would be preferred. Each phase current should be switched corresponding to machine back EMF as a function of the rotor position. At each rotor position, a constant current is multiplied by the constant part of the back EMF produces the output power of the machine.

III. MATHEMATICAL MODEL

Fig. 1 presents a single-phase equivalent circuit of the two-phase BLDC motor.

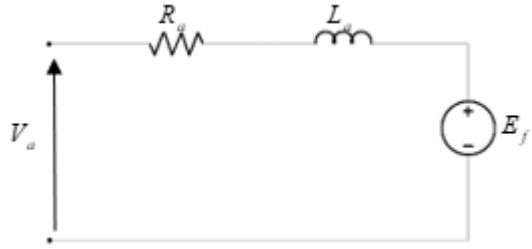

Fig 1. Equivalent circuit of a BLDC motor

The voltages of the two phases windings (va and vb) are as follows:

$$v_a = r_a i_a + \frac{d\psi_a}{dt} \tag{1}$$

$$v_b = r_b i_b + \frac{d\psi_b}{dt} \tag{2}$$

The flux-linkages of the phases (Ψ_a and Ψ_a) are as follows:

$$\psi_a = L_a i_a + \psi_{am} \tag{3}$$

$$\psi_b = L_b i_b + \psi_{bm} \tag{4}$$

From the above equations, the following matrix form equation are obtained:

$$\begin{bmatrix} v_a \\ v_b \end{bmatrix} = \begin{bmatrix} R_a & 0 \\ 0 & R_b \end{bmatrix} \begin{bmatrix} i_a \\ i_b \end{bmatrix} + \frac{d}{dt} \begin{bmatrix} L_a & 0 \\ 0 & L_b \end{bmatrix} \begin{bmatrix} i_a \\ i_b \end{bmatrix} + \frac{d}{dt} \begin{bmatrix} \psi_{am} \\ \psi_{bm} \end{bmatrix} \tag{5}$$

The flux-linkages rate of change, established by the PM at each phase, are equal to the induced back EMFs in the windings as follows:

$$\begin{bmatrix} e_a \\ e_b \end{bmatrix} = \frac{d}{dt} \begin{bmatrix} \psi_{am} \\ \psi_{bm} \end{bmatrix} \tag{6}$$

$$\begin{aligned} \psi_a &= K_w f\ (\theta_e) \\ \psi_b &= K_w f\ (\theta_e - \pi/2) \end{aligned} \tag{7}$$

The output power $P_{out,}$ input power P_{in} and the electromagnetic torque T_e are given by:

$$P_{out} = e_a i_a + e_b i_b \tag{8}$$

$$P_{in} = V_a i_a + V_b i_b \tag{9}$$

$$T_e = \frac{e_a i_a + e_b i_b}{\omega_{rm}} \tag{10}$$

And the mechanical equation is as follows:

$$T_e = J \frac{d\omega_{rm}}{dt} + B\omega_{rm} + T_L \tag{11}$$

where J is the inertia, ω_m is the shaft speed and T_L is the load torque. By referring to (8) and

(9), the input power is the product of the RMS values of current and voltage, and the output power is the product of the RMS value of the current and the back EMF.

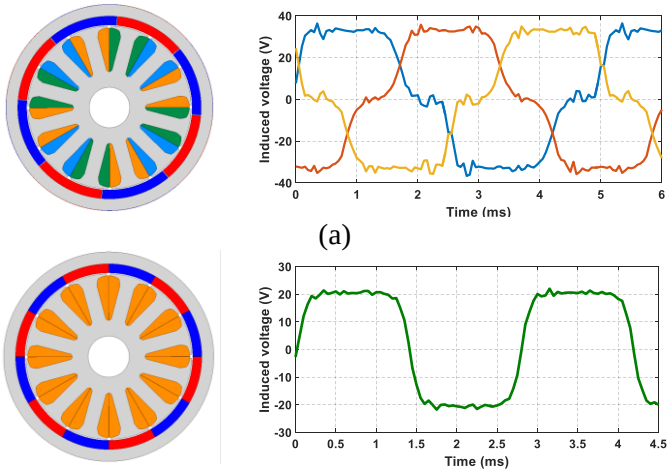

Fig. 2. Structure and back EMF of (a) three-phase BLDC motor (b) single-phase BLDC motor

In the conventional three-phase BLDC motor, the back EMF has an appropriate value about two-third of the period due to the structure of the rotor teeth and poles. Fig 2a shows a conventional BLDC motor with its back EMF. The stator current, which has contribution in generating the output power, should be applied in proportion to the back EMF. Otherwise, the supply voltage will drop on the resistance and inductance of the coil and a high current pass through the coils and inverter switches. This current is multiplied by a small amount of back EMF, and not only power will be generated, but it also causes additional losses and the need for more powerful electronics components. Therefore, to have back EMF in the entire interval, the flux-linkage of the PMs should be changed in the entire interval as shown in Fig 3. This is done only when the stator tooth width is equal to the rotor pole pitch. This is the structure of a single-phase BLDC motor in which due to the luck of the starting torque, it has not received much attention.

Fig 2b shows a single-phase motor with its back EMF. As seen, there is a back EMF almost over the entire range, so, the current can be passed over the entire range. In this case, all stator coils and cores are utilized simultaneously and the power has maximum value.

IV. DESIGN OF PROPOSED TWO-PHASE BLDC

In this section, the design procedure for two-phase dual stator BLDC motor is described. Two separate single-phase motors are designed. The first design is an internal rotor and the second design is an external rotor. It is noted that both motors have the same characteristics. After designing the two motors, they are collected together to form a dual stator motor. Using sizing equations and values listed in Table. 1, the motor design process is presented.

The diameter and length of the motor are calculated by the following output power equation. A trade-off must be made between the diameter and the length of the motor:

$$P_{out} = C_0 D^2 L\ n_s$$
$$C_0 = 1.11\ \pi^2 B_{av}\ ac\ k_w \quad (12)$$

where D, L and n_s are the average diameter, effective stack length and speed in rps respectively and B_{av}, ac and k_w, and are average flux density, specific electrical load and winding factor respectively. The rated RMS current (I_{rms}) is calculated considering the efficiency and voltage of the DC link. Because of the complete switching duty cycle, the DC link voltage is equal to the RMS of applied voltage V_{rms}:

$$P_1 = \frac{P_2}{\eta} = V_{rms} I_{rms} \cos\varphi$$
$$V_{rms} \approx V_{DC} \quad (13)$$

where $cos\ \varphi$ is the power factor. The cross section of the conductors, a, is calculated as:

$$a = \frac{I_{rms} . \sqrt{2}}{\delta} \quad (14)$$

where δ is current density. The thickness of PMs, h_{PM}, is calculated based on the desired flux density in the air gap as follows.

$$h_{PM} = \frac{B_{ag} L_{ag} \mu_{rPM}}{B_r - B_{ag}} \quad (15)$$

where B_{ag}, L_{ag}, μ_{rPM}, B_r are the air gap flux density, the air gap length, the magnet recoil permeability and the magnet remanent flux density respectively. Since the number of stator teeth is equal to and rotor poles, the slot pitch is used to determine the PM width and tooth width as follows.

$$\lambda = \frac{\pi D}{S_{teeth}} \quad (16)$$

$$W_{PM} = \frac{\pi D}{P} - X \quad (17)$$

where S_{teeth}, P and X are the number of stator teeth, the number of poles and the distance between PMs respectively. The dimensions of the rotor and stator core are calculated based on the appropriate flux density as follows:

$$T_{Wt} = \lambda - W_{slot} \quad (18)$$

$$T_W = \frac{B_{tip}}{B_{teeth}} T_{Wt} \quad (19)$$

$$L_{sbi} = \frac{B_{teeth}}{B_{sbi}} T_W \quad (20)$$

$$L_{rbi} = \frac{B_{teeth}}{B_{rbi}} T_W \quad (21)$$

where T_{Wt}, T_W, W_{slot}, B_{tip}, B_{teeth}, B_{sbi}, B_{rbi}, L_{rbi} and L_{sbi} are the teeth tip width, the tooth wide, the opening slot width, the tooth tip flux density, the tooth flux density, the stator yoke flux density, the rotor yoke flux density, the stator yoke length and the rotor yoke length respectively. At the end, after drawing the stator, the area of the groove (A_{eff}) is calculated and the number of coil turns (N_t) is obtained as follows:

$$A_{eff} = 0.4A_{slot}$$
$$N_t = \frac{\frac{A_{eff}}{2}}{a} \quad (22)$$

The external stator motor has larger average diameter and the same specifications of both motors are required, therefore, the PMs thickness and the coils number of turns of the second motor should be determined based on the features of the first motor. Table 2 summarizes the parameters and Fig. 3 shows the dimensions of the designed dual stator motor.

Table 1. Design data for two phase BLDC

Parameters	**Symbols**	**Values**
Rated power (kW)	P_{out}	4.5
Rated speed (rpm)	N_s	1000
Efficiency (%)	η	80%
Core material		M470-50A
Magnet Type		NdFe35
DC link voltage (V)	V_{DC}	50
Average flux density (T)	B_{av}	0.85
Specific electrical load	ac	20000
Winding factor	k_w	1
Power factor	$\cos\varphi$	0.75
Current density (A/mm^2)	δ	5
Air gap flux density (T)	B_{ag}	0.9
Air gap length (mm)	L_{ag}	1
Magnet recoil permeability	$\mu_{r_{PM}}$	1.04
Magnet remanent flux density (T)	B_r	1.24
Number of stator teeth	S_{teeth}	36
Number of poles	P	36
Distance between PMs (mm)	X	0.3
Wide of opening slot (mm)	W_{slot}	3.5
Flux density of teeth tip (T)	B_{tip}	0.9
Flux density of teeth (T)	B_{teeth}	1.8
Flux density of stator yoke (T)	B_{sbi}	1.2
Flux density of rotor yoke (T)	B_{rbi}	1.4

Table 2. Designed parameters in mm

Parameters	Symbols	Values	
Average radius of the first motor	R_1	130	mm
Average radius of the second motor	R_2	150	mm
Outer radius	R_{out}	185	mm
Inner radius	R_{in}	88	mm
Motor length	L	15	mm
cross section of the wires	a	5	mm^2
Thickness of first motor PM	h_{PM1}	1.8	mm
Thickness of second motor PM	h_{PM2}	1.3	mm
Arc of both motor PM	A_{PM}	10	deg
Wide of first motor teeth	T_{W1}	7.5	mm
Wide of second motor teeth	T_{W2}	8	mm
Wide of first motor teeth tip	T_{Wt1}	20	mm
Wide of second motor teeth tip	T_{Wt2}	24	mm
Length of both rotor yoke	$L_{rbi_{1+2}}$	15.5	mm
Length of first motor stator yoke	L_{sbi_1}	13	mm
Length of second motor stator yoke	L_{sbi_2}	11	mm
Number of coil turns	N_t	30	-
Number of coils	N_{coil}	36	-

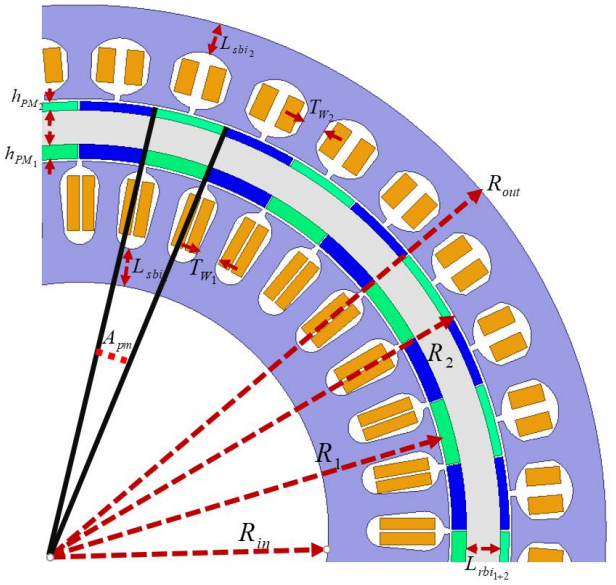

Fig. 3. Dimensions of the motor

V. SIMULATION

The complicated internal structure and nonlinear materials characteristics of the cores can be taken into account by FEM. The conventional 3-phase dual stator BLDC are simulated with

Ansys Maxwell and their control circuit, which includes inverter, source, etc., using twin builder Simplorer transient coupling, as shown in Fig. 5. Fig. 8 presents the two motors structure, which have the same characteristics such as dimensions, coils turn, the PMs volume and etc. The difference between the motors is the number of poles, the number of phases and the connection of the coils.

To use the same power supply for both inverters and creating the same conditions for windings of the motors, as shown in Fig. 4, each three windings of the conventional motor is divided into two groups connected in parallel. Also, each two coils of the proposed motor are divided into three groups that are connected in parallel.

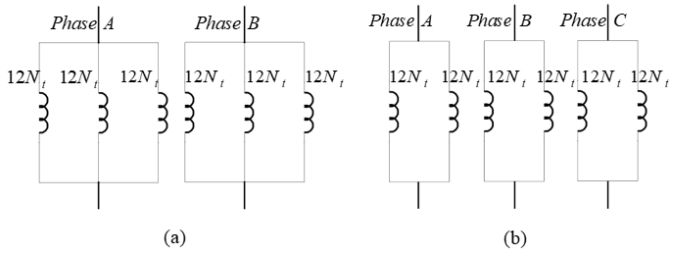

Fig. 4. Winding connections: (a) proposed two-phase BLDC motor, (b) conventional three-phase BLDC motor

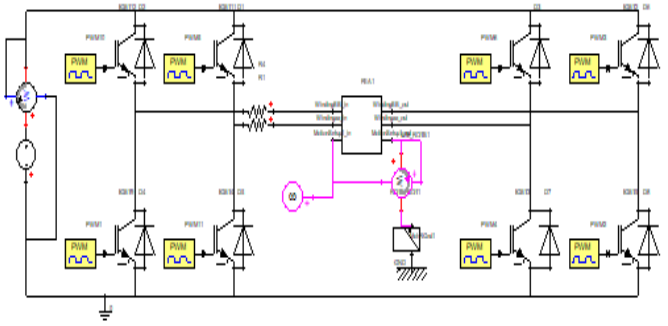

Fig. 5. Simplorer circuit for proposed motor

The proposed motor has two phases and therefore a higher number of turns. In addition, it has higher number of rotor poles and to have the same speed, the frequency will be higher. Therefore, Fig. 6 shows the phase difference between the current and its induced voltage developing a negative torque and decreasing the average torque. Therefore, in the high-speed operation, the advance angle is used to adjust the inverter switching. This is used here, and Fig. 7 shows the torque variations against advance angle. As seen, for higher advance angle, the average torque and its fluctuations increase, but to choose the appropriate angle, a trade-off must be made between the two. Based on the optimization, the chosen angle is 25^{0}.

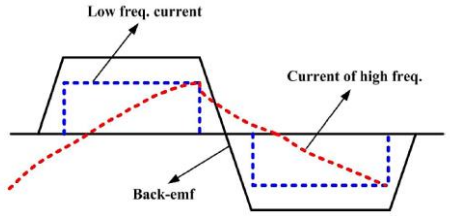

Fig. 6. Characteristics of phase current and back-emf waveform for low frequency and high frequency operation

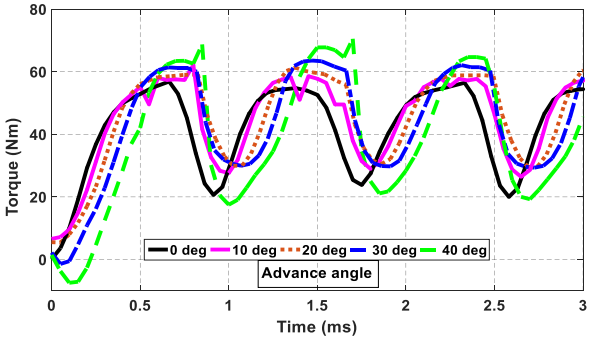

Fig. 7. Variations of torque against advance angle

VI. RESULTS AND COMPARISONS

Fig. 8 shows the structures, induced voltage, and current of the motors. According to the current and the induced voltage waveforms of the two motors, unlike the conventional type motor, it has value in the entire range, as mentioned above, with the presence of current and back EMF in the entire range, the current can be passed without any problem and it increases the developed torque and output power.

Fig. 9 shows the harmonic order of currents and voltages of two BLDC motor. As expected, the fundamental harmonic of the voltage in both motors is almost the same, but the fundamental harmonic of the current in the proposed motor is about twice that of the conventional motor. Considering the larger number of parallel coils in the proposed motor, as shown in Fig. 4, for having equal input power, the current should be 1.5 times. But the utilization of the complete duty cycle leads to an increase in the current. Therefore, with this design, the core, coils, and PMs are utilized more completely. The RMS of current and voltage of the proposed motor is 33 A and 105 V, respectively, and corresponding values for the conventional motor are 21 A and 81 V respectively.

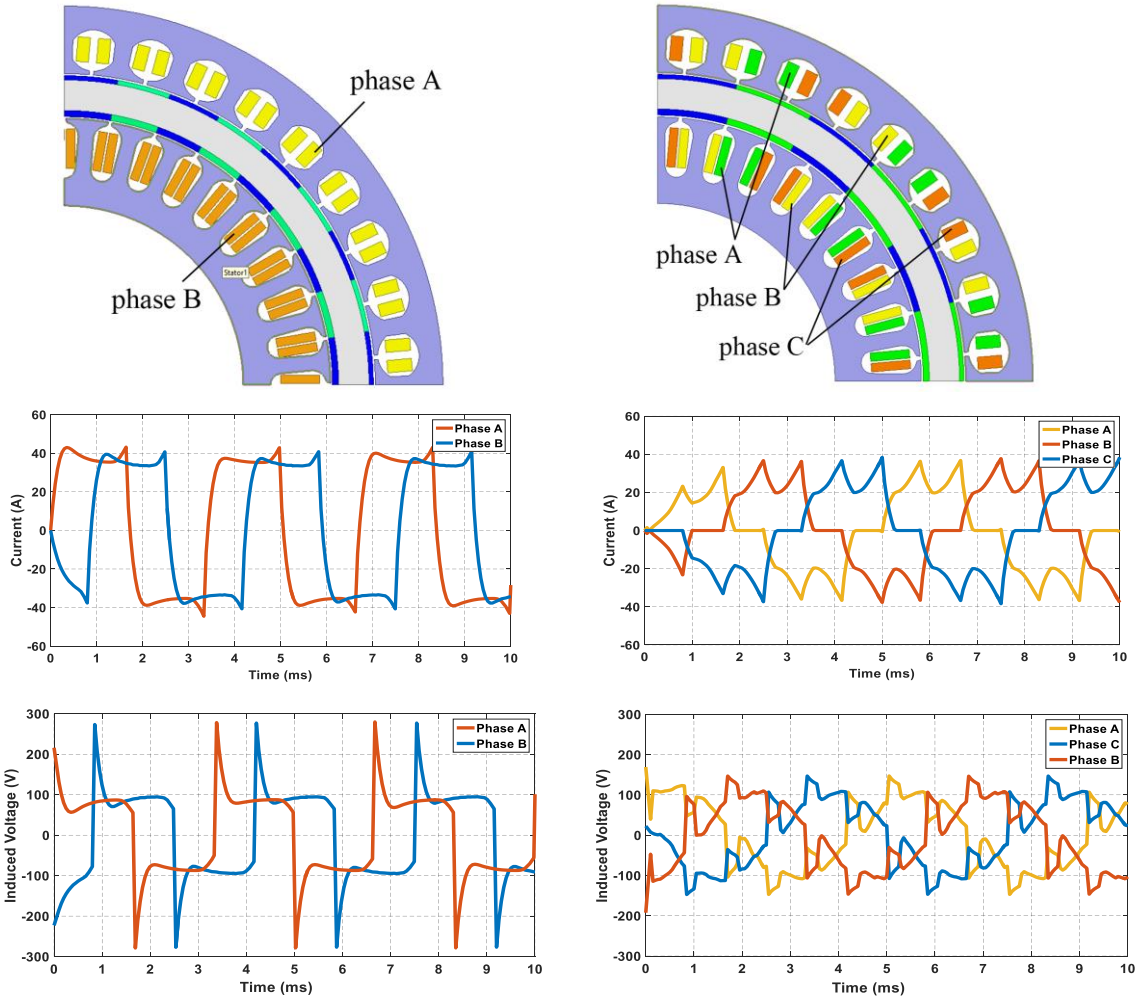

(a) (b)

Fig. 8. Structure, induced voltage and current of the (a) proposed two-phase BLDC motor, (b) conventional three-phase BLDC motor

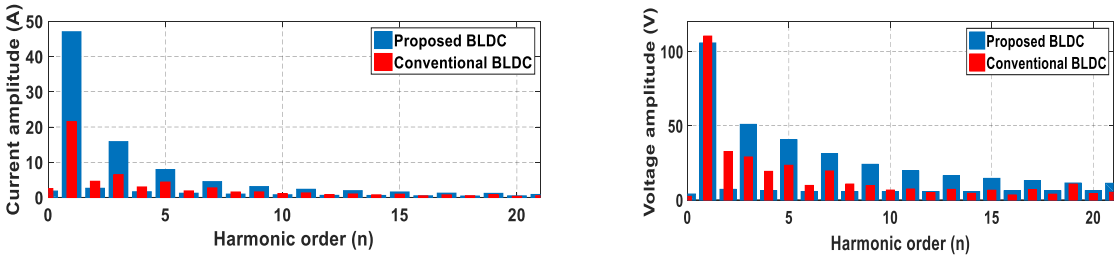

(a) (b)

Fig. 9. Harmonic order of the proposed and conventional BLDC motors: (a) current and (b) voltage

As shows in Fig. 10, the average torque and torque ripple of the proposed motor is 46 Nm and 65% respectively, and the corresponding values for the conventional three-phase motor is 32 Nm and 50% resectively. Fig. 11 shows the cogging torque of the motors, which is 22.3 Nm for the proposed BLDC and 18.25 Nm for the conventional BLDC.

The output powers of the proposed and conventional motors at the speed of 1000 rpm is 4.82 kW, 3.35 kW respectively. Therefore, the simulation also confirms the idea proposed in this paper, it means that at the same volume and dimensions, the torque and output power of the proposed motor is 1.43 times that of the conventional motor. Table. 3 presents the performance characteristics of BLDC motors for comparison.

Table 3. Performance characteristics of two BLDC motors

	Proposed BLDC motor	Conventional BLDC motor
Power (kW)	4.82	3.35
Speed (rpm)	1000	1000
Torque (Nm)	46	31
Voltage (V)	105	81
Current (A)	33	21
Power factor	0.75	0.7
Efficiency (%)	92	94

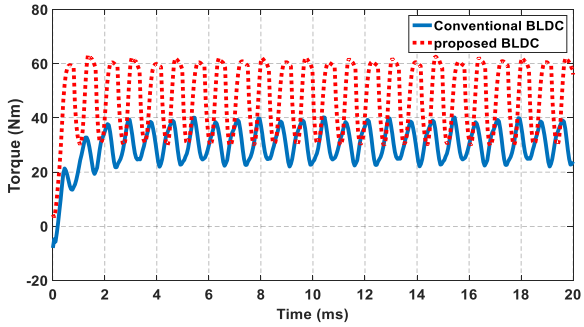

Fig. 10. Electromagnetic developed torque

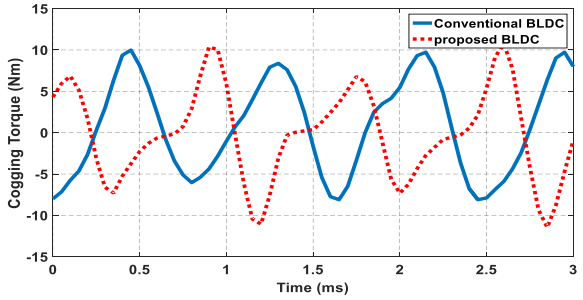

Fig. 11. Cogging torque

- Stator core loss

Stator core losses of both motors have been predicted by FEM under open circuit conditions and rated load. Table 4 presents the stator iron. As seen, the loss of the proposed machine is slightly higher than that of the conventional machine; however, considering the higher power of the proposed machine, this higher loss is acceptable. Besides, the stator core loss under the rated load is slightly higher than that of the open circuit case. The copper losses of the windings are neglected.

Table 4. Stator iron loss of motors

	Proposed motor		Conventional motor	
	Open circuit	rated load	Open circuit	rated load
Core loss	130	188	92	152
Eddy current loss	96	132	63.2	104

- Inverter

The windings of the two stator phases of the proposed motor must be independent, so, an inverter with 8 switches, as shown Fig. 5, should be used, which has two more switches compared to that of the conventional three-phase type.

VII. CONCLUSION

This paper proposed a new structure for two-phase BLDC motor. The advantage of this motor is its ability to receive a high energy or power, which has increased the torque density compared to other motors with the same size.

Higher torque is developed by this motor due to the duty cycle of the inverter switches, because unlike the conventional motors, these switches operate with a full duty cycle. Therefore, the windings and core are always directing the current and magnetic flux, which causes them to be used optimally and completely. In this paper, firstly, the mathematical model of the motor proved the method of increasing the developed torque, then, the desired motor was designed. The proposed motor was simulated by finite element analysis software and its optimal advance angle was selected to reach a reasonable torque. To show the higher torque density of this motor, a conventional three-phase dual-stator motor with the same dimensions and specifications were simulated. Finally, the comparisons show that the torque of the proposed motor is 1.43 times of that of the three-phase motor at the speed of 1000 rpm.

References

[1] B. Tibor, V. Fedak, and F. Ďurovský, “Modeling and simulation of the BLDC motor in MATLAB GUI,” Proc. - ISIE 2011 2011 IEEE Int. Symp. Ind. Electron., pp. 1403–1407, 2011, doi: 10.1109/ISIE. 2011.5984365.

[2] W. S. Im, J. P. Kim, J. M. Kim, and K. R. Baek, “Torque maximization control of 3-phase BLDC motors in the high speed region,” J. Power Electron., vol. 10, no. 6, pp. 717–723, 2010, doi: 10.6113/JPE.2010.10.6.717.

[3] S. Ahmed, “Investigations into the improvement of a single phase permanent magnetby ???”

2011.

[4] G. Cvetkovski, P. Lefley, L. Petkovska, and S. Ahmed, "Optimal design of a novel single phase PM BLDC motor using Genetic Algorithm," 15th Int. Power Electron. Motion Control Conf. Expo. EPE-PEMC 2012 ECCE Eur., pp. 1–8, 2012, doi: 10.1109/ EPEPEMC.2012.6397227.

[5] T. Yazdan, S. Atiq, B. Il Kwon, N. Baloch, and J. W. Kwon, "Two Phase Dual-Stator Axial-Flux PM BLDC Motor with Ironless Rotor Using Only-Pull Drive Technique," IEEE Access, vol. 7, pp. 82144–82153, 2019, doi: 10.1109/ACCESS.2019.2923711.

[6] T. Yazdan and B. Il Kwon, "Electromagnetic design and performance analysis of a two-phase AFPM BLDC motor for the only-pull drive technique," IET Electr. Power Appl., vol. 12, no. 7, pp. 999–1005, 2018, doi: 10.1049/iet-epa.2017.0709.

[7] K. Wang, Z. Q. Zhu, L. J. Wu, and G. Ombach, "Comparison of electromagnetic performance of 2- and 3-phase PM brushless AC machines for low speed applications," IET Conf. Publ., vol. 2012, no. 592 CP, pp. 10–15, 2012, doi: 10.1049/cp.2012.0280.

[8] V. Gholase and B. G. Fernandes, "Design of efficient BLDC motor for DC operated mixer-grinder," Proc. IEEE Int. Conf. Ind. Technol., vol. 2015-June, no. June, pp. 696–701, 2015, doi: 10.1109/ICIT. 2015.7125179.

[9] Gieras, Jacek F. "Permanent magnet motor technology: design and applications," CRC press, 2009.

[10] B. Boukais and H. Zeroug, "Magnet segmentation for commutation torque ripple reduction in a brushless DC motor drive," IEEE Trans. Magn., vol. 46, no. 11, pp. 3909–3919, 2010, doi: 10.1109/TMAG. 2010.2057439.

[11] R. R. Kumar, C. Chetri, P. Devi, and A. Dwivedi, "Design and analysis of dual stator dual rotor six-phase i-shaped permanent magnet synchronous motor for electric vehicles application," 9th IEEE Int. Conf. Power Electron. Drives Energy Syst. PEDES 2020, 2020, doi: 10.1109/PEDES49360.2020.9379763.

[12] Fazil M, Rajagopal KR, "Nonlinear dynamic modeling of a single-phase permanent-magnet brushless DC motor using 2-D static finite-element results," IEEE Trans. on Magnetics. 2011 Mar 22, vol. 47, no. 4, pp.781-6.

[13] S. Xia and S. Wang, "Design of high-speed high power density single-phase permanent magnet brushless dc motor considering control performance," Proc. IEEE Int. Conf. Ind. Technol., vol. 2020-Febru, no. 1, pp. 157–162, 2020, doi: 10.1109/ICIT45562.2020. 9067127.

[14] Z. H. Tang, Y. T. Chen, J. Luli, and R. H. Liang, "Analysis and Design of a Smart Startup Method for a Single-Phase BLDC Fan Motor," Electr. Power Components Syst., vol. 46, no. 16–17, pp. 1844–1856, 2018, doi: 10.1080/15325008.2018.1527867.

[15] W. Yaling and X. Yanliang, "A design study of dual-stator permanent magnet brushless DC Motor," Telkomnika, vol. 11, no. 4, pp. 653–660, 2013, doi: 10.12928/telkomnika.v11i4.1151.